ALMA MATER STUDIORUM
UNIVERSITÀ DI BOLOGNA

ARCHIVIO ISTITUZIONALE
DELLA RICERCA

Alma Mater Studiorum Università di Bologna
Archivio istituzionale della ricerca

A Highly Emissive Water-Soluble Phosphorus Corrole

This is the final peer-reviewed author's accepted manuscript (postprint) of the following publication:

Published Version:
Naitana, M.L., Nardis, S., Pomarico, G., Raggio, M., Caroleo, F., Cicero, D.O., et al. (2017). A Highly Emissive Water-Soluble Phosphorus Corrole. CHEMISTRY-A EUROPEAN JOURNAL, 23(4), 905-916 [10.1002/chem.201604233].

Availability:
This version is available at: https://hdl.handle.net/11585/600780 since: 2020-02-25

Published:
DOI: http://doi.org/10.1002/chem.201604233

Terms of use:

Some rights reserved. The terms and conditions for the reuse of this version of the manuscript are specified in the publishing policy. For all terms of use and more information see the publisher's website.

This item was downloaded from IRIS Università di Bologna (https://cris.unibo.it/).
When citing, please refer to the published version.

(Article begins on next page)

12 October 2024

This is the final peer-reviewed accepted manuscript of:

A Highly Emissive Water-Soluble Phosphorus, Corrole**,** Naitana, Mario L.; Nardis, Sara; Pomarico, Giuseppe; Raggio, Michele; Caroleo, Fabrizio; Cicero, Daniel O.; Lentini, Sara; Prodi, Luca; Genovese, Damiano; Mitta, Saisameera; Sgarlata, Anna; Fanfoni, Massimo; Persichetti, Luca; Paolesse, Roberto. CHEMISTRY-A EUROPEAN JOURNAL, 23 (4), 2017, 905-916.

The final published version is available online at: http://dx.doi.org/10.1002/chem.201604233

Rights / License:

The terms and conditions for the reuse of this version of the manuscript are specified in the publishing policy. For all terms of use and more information see the publisher's website.

This item was downloaded from IRIS Università di Bologna (https://cris.unibo.it/)

When citing, please refer to the published version.

Highly emissive water soluble phosphorus corrole

Mario L. Naitana,[a] Sara Nardis,[a] Giuseppe Pomarico,[a] Michele Raggio,[a] Fabrizio Caroleo,[a] Daniel O. Cicero,[a] Sara Lentini,[a] Luca Prodi,[b] Damiano Genovese,[b] Saisameera Mitta,[c] Anna Sgarlata,[c] Massimo Fanfoni,[c] Luca Persichetti,[d] and Roberto Paolesse*[a]

Abstract: The synthesis, spectroscopic and optical properties of the water soluble phosphorus complex of a 2-sulfonato-10-(4-sulfonatophenyl)-5,15-dimesitylcorrole have been investigated. The compound was prepared adopting a novel strategy for the corrole sulfonation, leading to the regioselective isomer in an almost quantitative yield. The phosphorus coordination has a “key role” in determining the corrole substitution pattern, limiting the formation of poly-substituted species, which affected the reaction of the corrole free base. The resulting complex shows excellent optical properties in terms of emission quantum yield, also in polar protic solvent, including water. ^{31}P NMR spectroscopy in CD_3OD indicates that the P sulfonate complex has been isolated in a hexacoordinated geometry with two different ligands (L1=-OH, L2=-OCH_3), and it is prone to axial ligand exchange with methanol, with no evidences of intermediate pentacoordinated species. The morphological characterization of thin layers of the P-corrole deposited onto Au(111) surface showed that the addition of an intermediate layer of reduced graphene oxide allows for a better control of corrole aggregation, inducing also transformation of the Au(111) reconstructed surface.

Introduction

Corrole can be considered the millennial porphyrinoid, since its chemistry has known a renaissance at the end of last century, when simple protocols for the synthesis of *meso*-triarylcorroles from simple commercial starting materials were reported.[1,2] Since these seminal works, the synthetic chemistry of corrole has been greatly improved thanks to the effort of different groups, and now yields similar to those of the parent porphyrin macrocycles have been obtained.[3]

This synthetic effort has been driven by the intriguing properties of corrole, which can be schematized as "similar, but different" than the corresponding porphyrin counterparts. Both the synthetic availability and the peculiar properties have paved the way for interesting applications of such a macrocycle, in fields ranging from catalysis, [4] clinical applications[5] to chemical sensors.[6]

The functionalization of the macrocycle has a critical role to optimize the corrole features for a specific application. Interestingly, these functionalizations have shown an unexpected regioselectivity, which allowed for the definition of a series of reaction pathways.[7]

In this promising scenario, one synthetic route is still quite elusive: the sulfonation reaction. This substitution has been very useful for the preparation of amphiphilic corroles but, unfortunately, this route has been successfully applied only to a single corrole derivative: the 5,10,15-tris(pentafluorophenyl)corrole.[8] For this corrole, the reaction regioselectively affords the corresponding 2,17-derivative in almost quantitative yields, opening the way for the exploitation of free base and metal derivatives of this corrole in several fields.[9]

Surprisingly, when the reaction was attempted to other similar corroles, the same regioselectivity was not observed and a complex, not separable mixture of different isomers was obtained, making the route of limited synthetic utility.[10]

In a previous work, we investigated in details the reason behind the unsuccess of this reaction,[11] since the preparation of the corresponding sulfonated corroles could be of great interest for further exploitations of such a macrocycle. We found that the apparent lower reactivity of 5,10,15-triphenylcorrole (**1**) with respect to the corresponding pentafluoro derivative is due to the much lower solubility of the first in the reaction conditions: the aggregation causes a slow dissolution of **1** and, consequently, the decomposition of the starting material.

Carrying out the reaction in CH_2Cl_2 avoided this drawback but, at the same time, we observed the formation of a series of regioisomers, confirming a not usual reactivity of corrole. In the series of products obtained (Scheme 1), we also identified the isocorrole **5**, which is the first stable tautomer of corrole. Thus, despite this study clarified the reason for the different reactivity of corroles in the sulfonation reaction, the problem of the reduced regioselectivity and synthetic interest was still not solved.

In this work we report a different route for the preparation of water soluble corroles, which, in the case of the phosphorus complex, allowed us to obtain a disulfonato derivative in good yields. The regioselectivity of the reaction has been demonstrated by NMR characterization, which evidenced also the axial ligand chemistry of the complex. The photophysical characterization of the complex showed brilliant emissive properties, particularly promising for practical applications. In view of these potential exploitations of the complex, we reported here also the

[a] Dr. M. L. Naitana, Dr. S. Nardis, Dr. G. Pomarico, M. Raggio, F. Caroleo, Prof. Dr. D. O. Cicero, Dr. S. Lentini, Prof. Dr. R. Paolesse
Dipartimento di Scienze e Tecnologie Chimiche
Università di Roma "Tor Vergata"
Via della Ricerca Scientifica 1, 00133 Rome (Italy)
E-mail: roberto.paolesse@uniroma2.it
[b] Prof. Dr. L. Prodi, Dr. D. Genovese
Dipartimento di Chimica "G. Ciamician"
Università di Bologna
via Selmi 2, 40126 Bologna (Italy)
[c] S. Mitta, Prof. Dr. A. Sgarlata, Prof. Dr. M. Fanfoni
Dipartimento di Fisica
Università di Roma "Tor Vergata"
Via della Ricerca Scientifica 1, 00133 Rome (Italy)
[d] Dr. L. Persichetti
Department of Materials
ETH Zurich
Hönggerbergring 64, Zürich 8093 (Switzerland)

morphological characterization of the P corrole thin layers deposited onto Au(111) surfaces.

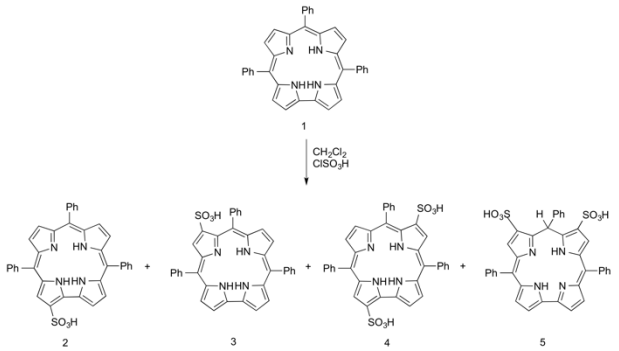

Scheme 1. Mixture of products obtained from the sulfonation of 5,10,15-triphenylcorrole.[11]

Results and Discussion

Synthesis

The lack of regioselectivity observed in the sulfonation reaction of triphenylcorrole led us to explore novel pathways for the preparation of sulfonato corroles, with the goal to orient the substitution reaction towards particular positions of the macrocyclic ring. Looking at the synthetic protocols developed for tetraarylporphyrins, one interesting reaction has been reported to obtain the regioselective functionalization of the peripheral meso-aryl rings: trimethylsilyl functionalized tetraarylporphyrins underwent a regioselective electrophilic substitution using the trimethylsilylchlorosulfonate $ClSO_3Si(CH_3)_3$ as sulfonating reagent, following the so called “organosilicon method” originally developed to obtain regiospecific disubstituted benzenes.[12] Besides, the application of this route to triarylcorroles is intriguing also for the possible functionalization of the peripheral aryl ring instead of the β-positions of the macrocycle, never obtained for corrole derivatives.

For this reaction, the trimethylsilyl functionalized triarylcorrole **6** was initially prepared and the sulfonation reaction was performed according the experimental conditions reported for tetraarylporphyrins. The result was a complicated mixture of water soluble poly-sulfonated corroles, in which spectroscopic characterizations evidenced a substitution pattern involving both the *para* phenyl and β-pyrrolic positions of the macrocycle. Once again corrole showed a high β-pyrrolic sensibility towards functionalization, nevertheless the results were promising, since a targeted substitution on phenyl ring could be achieved.

To study the reaction in details, we then decided to prepare the mono-substituted derivative **7**, obtained by reaction of the 4-trimethylsilyl benzaldehyde with two equivalents of mesityldipyrromethane,[13] following the reaction pathway reported in Scheme 2. The corrole was obtained in satisfying yields, slightly modifying the Gryko's route[14] by the optimization of the hydro-alcoholic solution composition.

The corrole was then reacted with $ClSO_3Si(CH_3)_3$, following the protocol reported in literature;[12] in a first attempt, a large excess of $ClSO_3Si(CH_3)_3$ was used and at the end of the reaction, the crude reaction mixture resulted to be soluble in water, indicating the formation of poly-sulfonated corroles. Thin layer chromatography showed the presence of several products, strongly suggesting the formation of different regioisomers. The reduction of the corrole/$ClSO_3Si(CH_3)_3$ ratio and variations of the reaction temperature were not satisfying and in all cases we obtained a mixture of water soluble corroles. However we could isolate a main reaction product, which resulted to be a trisulfonated corrole, in which the reaction occurred both at the meso phenyl and at the β–pyrrolic positions of the corrole ring. With the aim to regioselectively orient the reaction at the meso-phenyl position, we, therefore, further reduced the amount of $ClSO_3Si(CH_3)_3$, using only one equivalent of the reagent. In this case the reaction was not complete and some of the starting corrole **7** was recovered unreacted at the end of the reaction. The crude reaction mixture, however, was partially transferred to the aqueous phase and some products remained in the organic phase, thus indicating in this way the presence of mono-substituted products, while in the aqueous phase a disubstituted corrole was the main product.

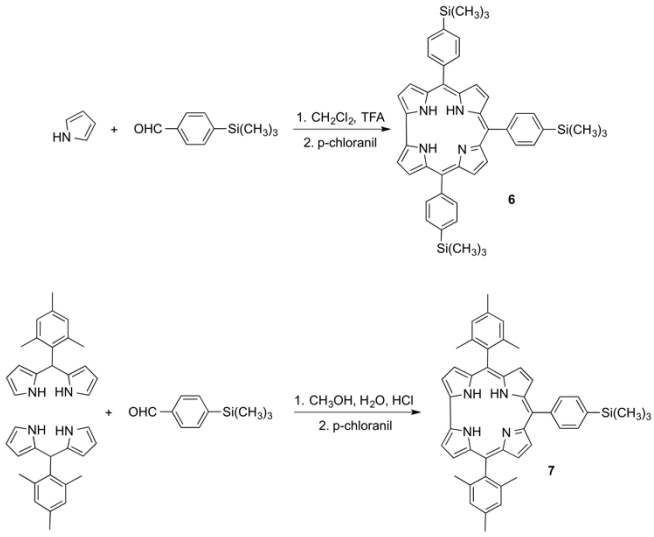

Scheme 2. Synthetic pathway for the preparation of **6** and **7**.

The chromatographic separation of the organic phase mixture allowed us to identify the compounds **8** and **9**, where the substitution was alternatively at the meso-phenyl and at the β-position. These two products were obtained in a 2/8 ratio, indicating that also in this case the β-pyrrolic positions were more reactive than the phenyl-silyl substituent. It is worth mentioning that the ^1H NMR spectroscopic data allowed us to identify the substitution of compound **9** in position 2 of the corrole ring, and no further mono-substituted isomers were isolated.

This feature can also explain the mixture of the different products obtained in the case of trimethylsilyl chlorosulfonic acid excess,

as reported in Scheme 3. The sulfonatophenyl corrole undergoes the substitution at the β-pyrrolic positions, giving a huge number of possible different regioisomers.

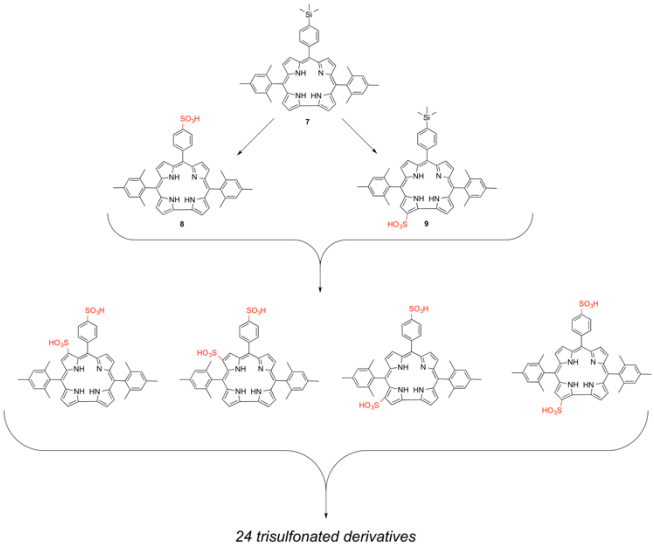

Scheme 3. The reaction steps for the formation of different isomers from the sulfonation reaction of **7**.

This result confirmed that the high reactivity of the corrole β-pyrrolic positions hampers the possibility to obtain a regioselective substitution, consequently limiting the synthetic utility of this route. The key to overcome this drawback is to reduce the reactivity of the corrole macrocycle. One possibility is to carry out the reaction on a corrole metal complex, since the coordinated metal can both increase the macrocycle stability and reduce its reactivity.

Among the different corrole derivatives, we decided to explore the reactivity of the phosphorus complex. The choice of this complex is due to the different reactivity showed by this derivative in the β-functionalization of corrole, such as for example the nitration reaction.[15] Generally the nitrating reagent of choice for this reaction is a mixture of $AgNO_2$ and $NaNO_2$: the silver ion is needed to oxidize the corrole ring, which then undergoes the nucleophilic attack of the nitrite ion to give the desired β-nitro corrole. We recently reported that P corrole is not reactive in these conditions: the P(V) ion reduces the electron density of the corrole ring, making then not possible its oxidation. [15] In this case we had to use the electrophilic route, using $LiNO_3$ or $NaNO_3$ as nitrating reagents; in both cases, however, the reaction yields were lower than those usually obtained for other metal complexes of corroles, confirming again the ability of the coordinated P(V) to reduce the corrole electron density.[16]

In our case, the ability of P to reduce the corrole ring reactivity in electrophilic substitutions could be of help to increase the reaction of the peripheral phenyl ring, and to control the reaction regioselectivity (the site of macrocycle functionalization). A limitation of the scope of this approach could be the absence of protocols for the demetalation of P corroles, which cannot allow the possible preparation of both free base or other metal complexes of sulfonated corroles; on the other hand, this route could be a case study with potential extension to other metal complexes of corrole.

The reaction of **7** with $POCl_3$ in boiling pyridine afforded the P complex **10** in high yields. The sulfonation reaction was initially attempted with one equivalent of the $ClSO_3Si(CH_3)_3$, in the same conditions as the free base reaction. In this case, however, the complex was not reactive and **10** was quantitatively recovered after 4 hours of reaction. This result indicated that the P coordination effectively reduces the reactivity of the corrole toward the sulfonating agent. We then increased the amount of the reagent to 1:3 ratio, and in this case we immediately observed the formation of products. After 2 hours, the reaction did not proceed further and the reaction work up showed that the crude mixture was distributed both in the organic and in the aqueous phase, indicating the formation of mono- and poly-sulfonated corroles.

The separation of the organic phase showed the presence of the starting material **10** as the major component and two further fractions in similar amounts (3% yield), which were separated by chromatography.

The spectroscopic characterization indicated that these compounds were the mono-sulfonated corroles **11** and **12**, in which the sulfonation occurred at the meso-phenyl or at the β-position. In the aqueous phase a single product was evidenced, namely a disulfonated species, with the sulfonic groups simultaneously present both at the meso-phenyl and at the β-pyrrolic positions.

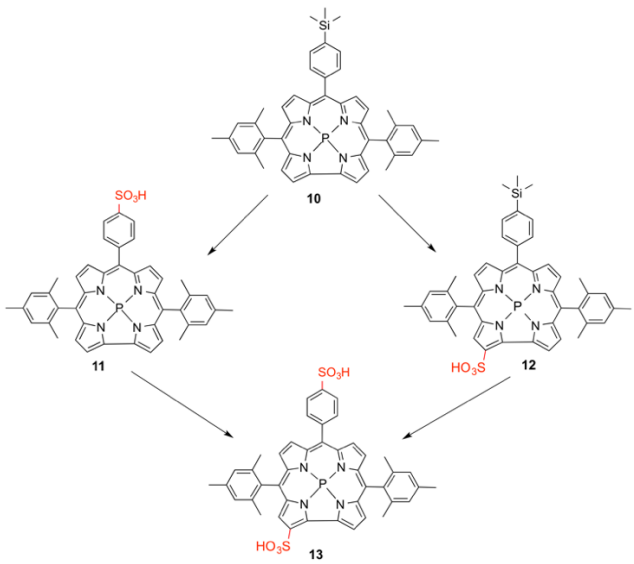

Scheme 4. The synthetic route leading to **13** (P axial ligands omitted for clarity).

We further increased the amount of the $ClSO_3Si(CH_3)_3$ to 1:5, carrying out the reaction in the same conditions. In this case **10** reacted completely and only traces of the mono-substituted products were present in the organic phase during the reaction

work-up, while the crude mixture was almost quantitatively distributed in the aqueous phase. No chromatography was necessary for the separation of the product present in the aqueous phase, which was dissolved in methanol and purified by filtration over silica pad to remove the salts excess. The mass spectrum of this product indicated the formation of a disulfonated species **13**, in which the substitution occurred at the β-pyrrolic position and at the meso-phenyl ring, as indicated by the absence in the ^{1}H NMR spectrum of the resonances of the trimethylsilyl group (Scheme 4). This compound was obtained in an almost quantitative yield.

To unambiguously determine the regioselectivity of the reaction, we tried to perform the X-ray crystallographic characterization of **13**, but unfortunately all the attempts to obtain single crystals of this compound by slow crystallization from CH_3OH/CH_2Cl_2 were unsuccessful. For this reason, the characterization of **13** was done by a detailed ^{1}H NMR study.

NMR Spectroscopy.

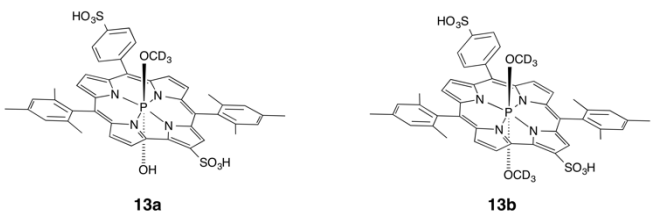

Figure 1. The molecular structure of the reaction products.

In literature the characterization of P corroles evidenced the facile substitution of the axial ligands in the presence of coordinating solvents.[17] This feature is also confirmed in the case of **13**, as indicated by the FAB mass spectrum, where the molecular peak corresponds to **13** bearing as axial ligands two 3-nitrobenzyl alcohols, the matrix used for the FAB analysis. To avoid the presence of different species in solution, we decided to record ^{1}H and ^{31}P NMR spectra of **13** in CD_3OD, with the aim to obtain exclusively **13b** (Figure 1) in solution. However, in the freshly prepared solution of **13** in CD_3OD, we clearly detected the presence of two different species (Figure 1).

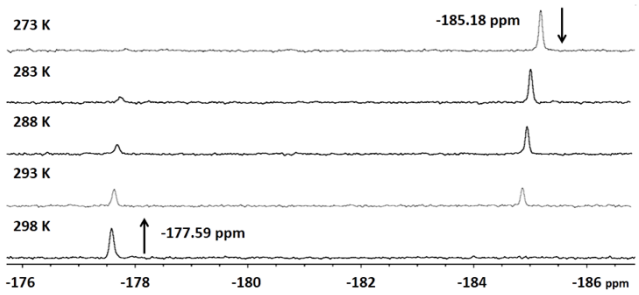

Figure 2. Comparison between ^{31}P NMR spectra of compound **13** at different temperature in CD_3OD.

The dependence on temperature of the relative ratio reflects the change in the interconversion kinetics (Figure 2). For instance, a freshly prepared sample of compound **13** shows a single ^{31}P signal (at -185.18 ppm) at 273 K; the other signal belonging to the other species (-177.59 ppm) appears at 283 K, reaching an equimolar content at 293 K. At the final temperature of 298 K, the original species is completely converted into the other one.

Sensitive difference in ^{31}P chemical shift value of the two species suggests that a strong change on the coordination environment of phosphorus center could be taking place.[17] As a confirmation of such evidence, a previous spectroscopic study of phosphorus(V)-*meso*-triarylcorrole derivatives[17c] highlights that the hexacoordinated species with two hydroxyl groups in the axial positions was prone to axial-ligand dissociation to form the corresponding pentacoordinated complex. However, in the presence of strongly coordinating solvents, the hexacoordinated geometry is stabilized by replacing the axial OH ligands with more strongly bound methoxy groups.

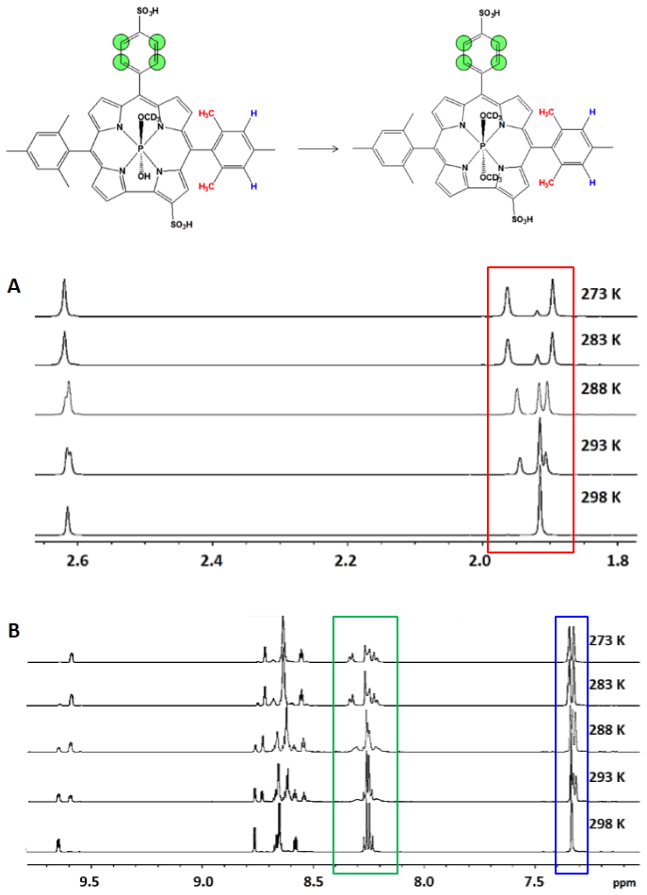

Figure 3. Comparison between ^{1}H (**A**, aliphatic region; **B**, aromatic region) NMR spectra of compound **13** at different temperature in CD_3OD.

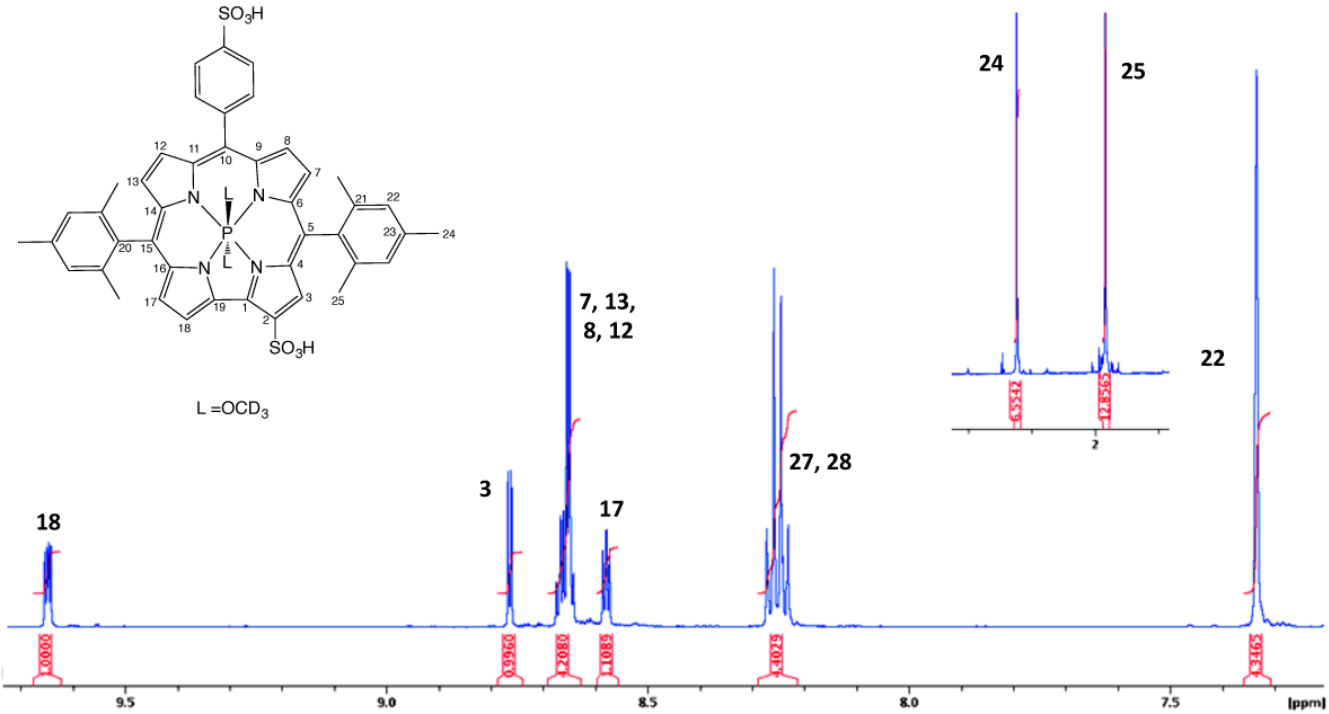

Figure 4. ^{1}H NMR assignment of compound **13b** (solvent CD_3OD). See Table S1 for the complete list of chemical shifts

Under our experimental conditions, using methanol as solvent, we were unable to observe pentacoordinated species. The two ^{31}P chemical shift values are compatible with two hexacoordinated species containing one (**13a**) and two (**13b**) -OCD_3 groups, in the axial positions respectively. The ^{31}P chemical shift strongly suggests that **13a** contains an OH and an OCD_3 as axial ligands. At 273 K compound **13a** begins to convert into **13b** after 1 hour from dissolution in methanol; while at 293 K the conversion is mostly complete within 25 minutes (Figure S9).

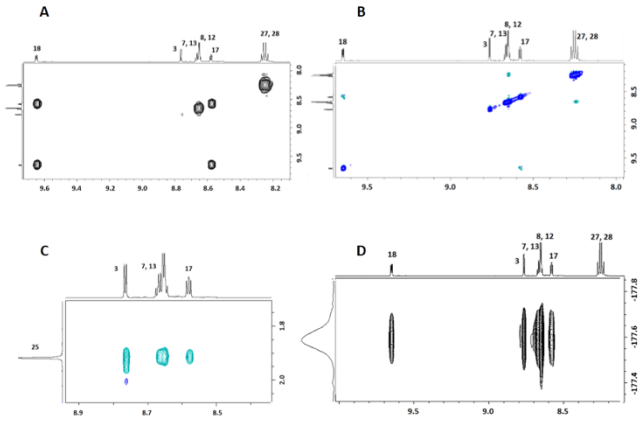

Figure 5. ^{1}H-^{1}H COSY and ROESY spectra (A, B and C) and ^{1}H-^{31}P HSQC spectrum (D) of compound **13b** (aromatic region) in CD_3OD.

Also the ^{1}H NMR spectra recorded at variable temperature showed a progressive conversion of compound **13a** into **13b**, resulting in a loss of asymmetry. The presence of two *ortho* methyl groups in 5, 15-*meso*-mesityl moieties greatly increases the activation energy of the rotational barrier around the aryl-macrocycle bond, thus preventing their rotation. As a consequence, no thermal isomerization was observed under the experimental conditions used.

Therefore, at low temperature *ortho* methyl group in **13a** is split into two different resonances, reflecting two different orientations toward the non-symmetrical plane of the molecule, due to the presence of the two different axial ligands (Figure 3A, marked in red); as the temperature is increased, the formation of symmetrical compound **13b** gives rise to a single signal. The same behavior could be observed for the two aryl protons (Figure 3B, marked in blue).

On the other hand, the 10-*meso*-phenyl ring, characterized by a lower rotational barrier, shows a more complex NMR pattern depending on temperature, being the outcome of the simultaneous conversion of **13a** into **13b** together with the contribution of dynamic conformational exchange (Figure 3B, marked in green).

2D NMR experiments were performed at 298 K to confirm the structure of compound **13b** and unambiguously assign the positions of sulfonic substituents. As observed in the ^{1}H NMR spectrum (Figure 4) the presence of seven β-pyrrolic signals indicates a monosubstitution on the corrole macrocycle.

A combination of ^{1}H-^{1}H ROESY and COSY experiments confirmed that the sulfonic substituent is placed in position 2, as indicated by the absence of NOE between pyrrole-pyrrole bridge protons (Figures 5A and 5B). Moreover ROESY cross peaks detected for the *ortho* methyl groups allowed to assign all the β-pyrrolic protons adjacent to the mesityl portions (Figure 5C). In addition, NOEs between β-pyrrolic protons 8 and 12 and the *ortho* protons belonging to the sulfonatophenyl ring are clearly visible

(Figure 5B). In the ^{1}H-^{31}P HSQC spectrum (Figure 5D), phosphorus shows scalar coupling with the β-pyrrolic protons. This is reflected in the multiplicity of β-pyrrolic signals, such as protons 3 being a doublet. Finally, ^{1}H-^{13}C HSQC and HMBC experiments are consistent with the reported structure; in particular, ^{13}C chemical shift values of 10-*meso*-phenyl ring are compatible with a *para* sulfonic-substituted phenyl group.

Photophysical characterization

The P complexes of corrole have been reported to have exceptional properties within the class of dyes based on this macrocycle, in particular with high fluorescence quantum yields in the range of 0.21-0.68.[17b,18] The P-corrole **13** confirms these feature, it is moderately soluble in water and very soluble in methanol, and in both solvents it features a very high brightness, as a result of the large values of molar extinction coefficient and of photoluminescence quantum yield (Φ□= 0.24 in methanol and Φ = 0.26 in water, Table 1).

The absorption spectrum of **13** in methanol features indeed an intense Soret-like band with two narrow peaks centered at 410 and 420 nm (ε = 69000 $M^{-1}cm^{-1}$ and 76300 $M^{-1}cm^{-1}$ respectively, Table 1, Figure 6), and a set of Q-like bands showing an intense peak at 599 nm (600 nm in water).

Table 1. Photophysical properties of 13.

Solvent	$\lambda_{max,Abs}$/nm	ε_{max}□/ $M^{-1}cm^{-1}$	$\lambda_{max,Em}$/nm	QY%	τ / ns	k_r /10^6	k_{nr}/ 10^9
CH_3OH	420	76300	604	24	3.3	72.7	0.23
CH_3OH, 77K			600		4.7		
H_2O[a]	419	65240	604	26	3.6	72.2	0.21

[a] Solution prepared by dispersing 50 μL of a concentrated CH_3OH solution in 3 mL H_2O.

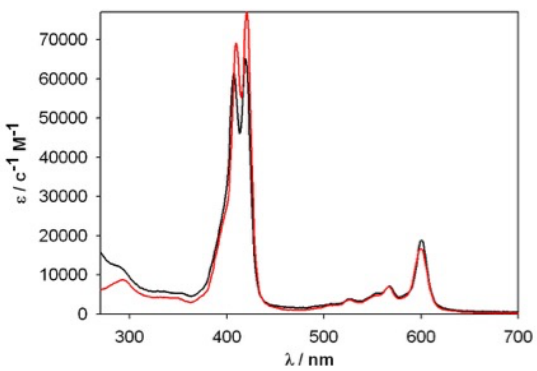

Figure 6. Molar extinction coefficient spectra of **13** in methanol and in water (red and black lines respectively).

The excitation spectra, both in methanol and in water, match very well the absorption spectra, indicating that the emissive state is formed regardless of the excitation wavelength (Figure 7). Similar results in terms of emission and excitation spectra were observed at 77 K, with a slightly longer excited state decay (τ = 4.7 ns) (Figure S12), indicating that, as for other corroles,[19] a thermal non radiative deactivation pathway is active at room temperature. No emission was observed in the 800−1600 nm region –nor at room temperature nor at 77 K– indicating a negligible efficiency for phosphorescence or for singlet oxygen sensitization under all experimental conditions.

In conclusion, the P-corrole reported in this study displays very good photophysical properties, owing to its high quantum yield of emission in the red region of the visible spectrum, associated to an intense and sharp-peaked absorption spectrum. Thanks to such properties and to a negligible formation of reactive oxygen species upon irradiation, we foresee large and multidisciplinary interest in this compound, also considering its unique solubility in polar protic solvents including water.

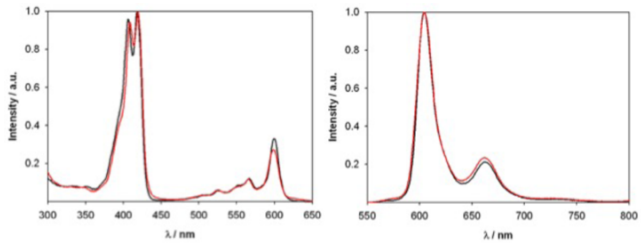

Figure 7. Excitation (left, λ_{emis} = 670 nm) and emission (right, λ_{exc} = 410 nm) spectra of **13** in methanol and water (red and black lines respectively).

Scanning Tunneling Microscopy (STM) Characterization.

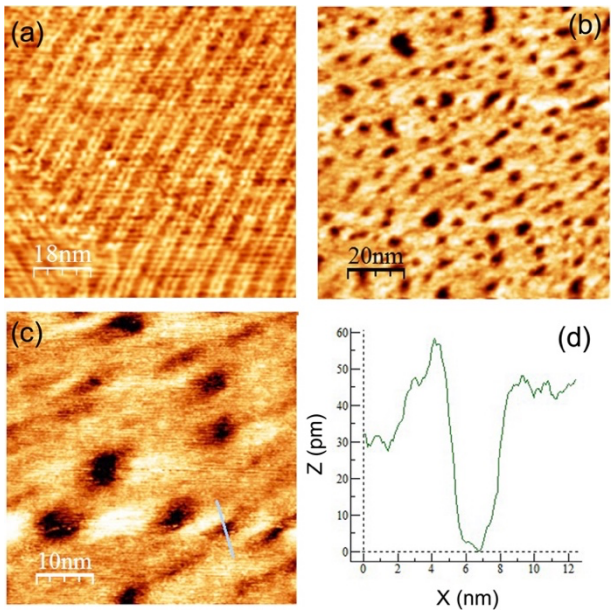

Figure 8. STM images (I=1 nA and V=0.2V) of: (a) (90x90nm^2) clean herringbone reconstructed Au(111) surface. After corrole deposition with spray coating: (b) (100x100nm^2); (c) (50x50nm^2); (d) depth profile along the line reported in (c)

The interesting properties of **13** led us to study the morphology of thin films of this macrocycle deposited onto gold surfaces, which could give interesting insights for future applications of this compound, for example, as chemical sensor. We demonstrate phosphorus-centered-corrole molecule interaction with reduced graphene oxide on Au (111) surface supported-system.

We first prepared a clean and reconstructed single crystal Au(111) by using annealing cycles in air at room temperature. Onto this herringbone reconstructed Au(111) surface (Figure 8a) we deposited the corrole molecules from a methanol solution using the spray coating technique. This technique has been widely used for the functionalization of chemical sensors, since it is rather simple and allows a fine tuning of the amount deposited onto the surface by varying the spraying time as well as the solution concentration.

At low amount of the sprayed corrole, STM characterization of the Au(111) surface showed that the macrocycles form a film which is not complete, but presents vacancies leading to formation of pits (the dark spots in the Figure 8b,c) randomly distributed throughout the surface. The average depth of the pit ranges from 60 pm to 80 pm (see Figure 8d) indicating that corrole rings lay almost parallel to the surface.[20,21]

This kind of pits was also reported for corrole dimers sprayed onto Au(111) surface[22] as well as when alkane thiols[23,24] were adsorbed on the Au surface. However, a different mechanism is operating for the formation of these pits: in the case of alkane thiols, the holes are formed directly on the Au surface because the strong thiol interaction with gold corrodes the metal surface. Therefore the depth of the pits is equivalent to the monoatomic step of Au(111) surface (0.24nm). In the case of the corrole layer, however, the pits are formed by molecular vacancies on the film previously deposited on the Au surface as our results confirm due to the over layer thickness.

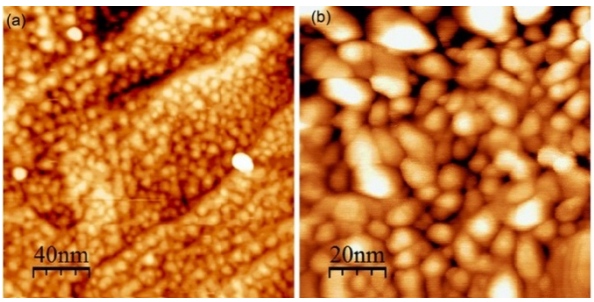

Figure 9. STM images (I=1 nA and V=0.2V) of corrole molecular aggregations deposited on Au (111) surface using drop casting method. Scan area: (a) 200×200nm^2, (b) 100×100nm^2

The surface morphology changes when the corrole layer is deposited by another deposition method, i.e. by drop casting. In this case the formation of aggregates on the Au surface was clearly evident in the STM images (Figure 9). The strong tendency of corrole to π-π interact leads to the formation of aggregates upon increasing macrocycle concentration. Previous results[21] report a similar behavior in the case of high molecules concentration.

With the aim to investigate a possible way to increase the interaction of corrole with the surface, we decided to use Reduced Graphene Oxide (RGO) as intermediate layer, on which we deposit the P corrole complex. The axial oxygen ligand exchange of P corroles, as evidenced by the NMR characterization, can be a promising tool to graft the corrole onto the RGO, where some OH groups are present. For this reason, initially we deposited only RGO on a freshly-prepared Au(111) surface and after RGO deposition we observed some strong morphological effects (see SI for details).

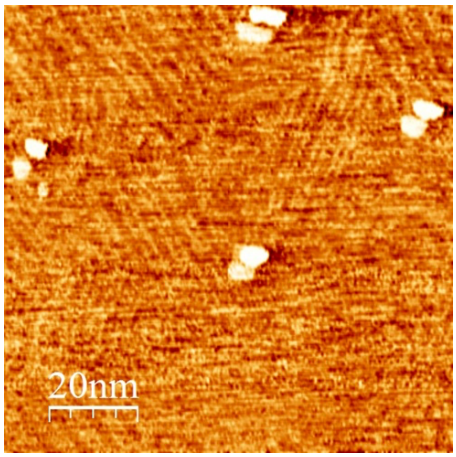

Figure 10. STM image (I=1 nA and V=0.2V) (100x100nm^2) of Au(111) surface after RGO and corroles deposition. Small molecular aggregations that tend to follow the substrate corrugation lines of herringbone reconstruction are evident

Upon deposition of corrole and RGO mixed solution on the freshly-prepared gold surface by spray coating technique, surface modifications were observed. The first evidence is the appearance on the flat gold planes of small molecular aggregations. These clusters tend to follow the substrate corrugation lines of herringbone reconstruction, as shown (Figure 10).

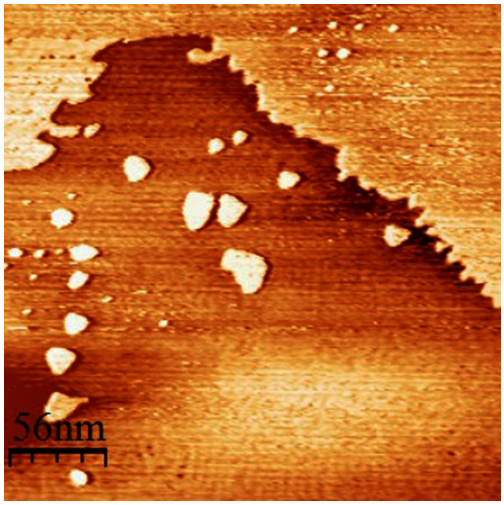

Figure 11. STM image (I=1 nA and V=0.2V) (280x280nm^2) of Au(111) surface after RGO and corroles deposition. Large clusters on flat terraces along with "tooth like" structures near the step edges are evident.

These small aggregates represent the early stage of larger clusters that form on flat terraces, while, near the step edges, "tooth like" structures appear (Figure 11) giving rise to the formation of nano fingers.

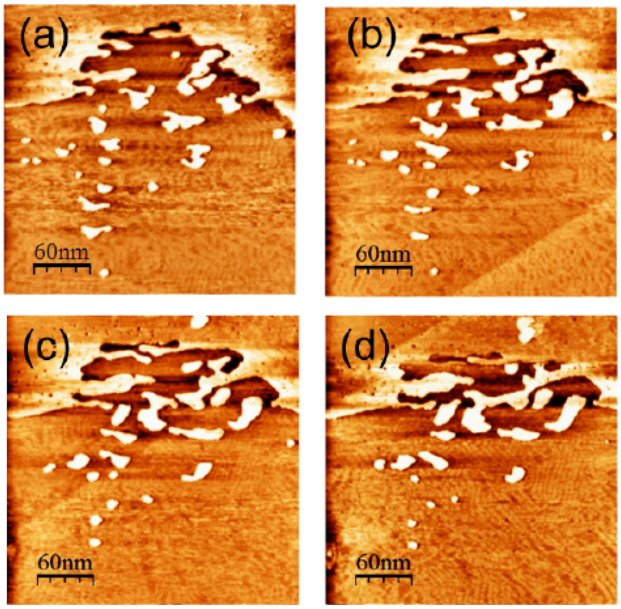

Figure 12. From (a) to (d) successive recorded STM images (I=1 nA and V=0.2V) (300x300nm^2) of Au(111) surface after RGO + corrole deposition. A very high mobility of the structures induced by STM scans is clear.

All the aggregate structures on the surface are not stable. An extraordinary mobility of these clusters was captured through a series of STM images (Figure 12). Multiple images were acquired on the same region by repeated scans of the STM tip. The tip induced modifications of the surface are evident.

Such high mobility, which is also reported in similar systems,[25] explains the difficulty to image individual molecules in our experimental conditions.

Different kind of interactions can contribute to the atomic displacement and it is difficult to identify the mechanism at atomic level, however we can hypothesize that RGO and corrole lower the energy barriers for Au atom detachment for step edges, leading to the formation of nanofingers as well as the very high mobility of clusters. Similar behavior was observed when only RGO is deposited on Au(111) surface (see SI).

Conclusions

Because of their peculiar properties, corroles are finding important applications in fields such as catalysis, sensing and medical therapy, competing in this sense with the more common class of porphyrins. In this promising scenario, one synthetic route for the preparation of corroles is still quite elusive, e.g., the sulfonation reaction. This substitution could be potentially very useful for the preparation of water soluble corroles but until now has been successfully applied only to a single corrole derivative: the 5,10,15-tris(pentafluorophenyl)corrole. In this context, we have developed a new synthetic strategy, based on phosphorus coordination, for obtaining **13** in an almost quantitative yield, paving the way to an even broader use of this reaction on corrole derivatives.

Interestingly, **13** displays very good photophysical properties even in water solution, and in particular a high fluorescent quantum yield in the red region associated with the intense absorption bands typical of the porphyrinoid systems. For these reasons, **13** is particularly appealing for the design of highly efficient fluorescent labels and sensors.

For these applications it is usually important to deposit the chromophore onto metallic surfaces. In view of this, we have characterized the morphology of **13** thin films by STM and we identified the transformations of the reconstructed surface of an Au (111) single crystal occurring when corroles are deposited in air at ambient temperature. We have shown that the strong π-π interaction between corroles compared to the weak interaction with the gold substrate is better controlled in the case of spray casting deposition method and depositing a layer of RGO along with corroles. The presence of the RGO lowers the energy barrier for the detachment of gold atoms from step edges at room temperature, producing a very high mobility of the structures resulting in formation of nano fingers, even under low-field conditions.

Experimental Section

Materials. Silica gel 60 (70–230 mesh, Sigma Aldrich) was used for column chromatography. Reagents and solvents (Aldrich, Fluka) were of the highest grade available and were used without further purification. Room temperature ^{1}H NMR and ^{31}P spectra were recorded with a Bruker AV300 spectrometer operating at 300.13 MHz (^{1}H) or at 121.48 MHz (^{31}P). Chemical shifts are given in ppm relative to residual solvent ($CHCl_3$ 7.26 ppm, CH_2Cl_2 5.32 ppm) for ^{1}H and to a $CDCl_3$ solution of PPh_3 (-6.1 ppm) as external standard for ^{31}P. 1-bromo-4-(trimethylsilyl)benzene, 4-trimethylsilylbenzaldehyde and mesityl-dipyrromethane were synthesized according previous reported literature procedures. [12,13,26]

NMR measurements. ^{1}H and ^{31}P spectra were recorded with a Bruker Avance 600 MHz spectrometer operating at 600 MHz for ^{1}H and 243 MHz for ^{31}P, equipped with a 5 mm inverse broad band BBi probe and z-axis gradients. All experiments were performed in CD_3OD at different temperature. 2D NMR experiments were recorded at 298 K. ROESY spectrum were acquired with a spectral window of 6.3 kHz (carrier frequency at 4.75 ppm) using 4096 t_2 data points (512 t_1 increments), 4 transients with relaxation delays of 2 s and a mixing time of 800 ms. COSY spectrum were collected with a spectral window of 6.3 kHz (carrier frequency of 4.75 ppm) using 4096 t_2 data points (256 t_1 increments), 4 transients with relaxation delays of 2 s. ^{1}H-^{13}C HSQC experiment were acquired with a spectral window of 7.5 kHz and a carrier frequency at 125 ppm using 4096 t_2 data points (256 t_1 increments), 8 transients with relaxation delays of 2 s. ^{1}H-^{13}C HMBC experiment were acquired with a spectral window of 30 kHz (carrier frequency at 100 ppm) using 4096 t_2 data points (1024 t_1 increments), 16 transients with relaxation delays of 2

s. ^{1}H-^{31}P HSQC experiment were acquired with a spectral window of 1.9 kHz and a carrier frequency at -178 ppm using 2048 t_2 data points (256 t_1 increments), 4 transients with relaxation delays of 2 s. All data were processed with TopSpin.

Photochemical measurements. UV-VIS absorption spectra were recorded at 25°C with Perkin-Elmer Lambda 45 spectrophotometer. The emission and excitation spectra were recorded with a modular UV-vis-NIR spectrofluorimeter Edinburgh Instruments FLS920 equipped with a photomultiplier Hamamatsu R928P. The latter instrument connected to a PCS900 PC card was used for the Time Correlated Single Photon Counting (TCSPC) experiments. Quartz cuvettes were used for both absorbance and emission measurements (optical path length of 1 cm). Luminescence quantum yields (uncertainty ± 15%) were recorded on air-equilibrated solutions using tetraphenylporphyrin (Φ = 0.11) in de-aerated toluene as reference dye.[27] Corrections for instrumental response, inner filter effects and phototube sensitivity were performed.[28]

STM measurements. STM measurements were performed in air at room temperature using WA technology TOPS system. Electrochemically etched W tips were used for the STM measurements. All the images were acquired at constant current mode. The deposition of corrole onto Au(111) crystal surface was carried out by spray casting method, using a 0.01 mg/mL water solution of **13**. A Graphene Oxide (GO) layer was deposited by spray casting method, starting from a 0.01 mg/mL suspension of the GO in water. After deposition, the Au surface was put in a beaker with 0,5 mL of a 50-60% hydrazine aqueous solution on a water bath. The temperature was regulated at 95 °C for an hour and then the sample was left to cool down to obtain the RGO layer. To produce the mixed **13**/RGO layer a GO/corrole solution was prepared by mixing a designated volume of GO suspension (0.2 mg/mL) and corrole solution (0.1 mg/mL) to obtain a 1:4 w/w GO corrole ratio. After spray coating deposition the surface was treated with hydrazine to obtain the RGO layer.

5,10,15-tris(4-trimethylsilyl)corrole 6. Corrole synthesis was performed on the basis of published procedure.[29] Pyrrole (2.8 mL, 40mmol), 4-trimethylsilylbenzaldehyde (4.2 mmol, 740 mg) and trifluoroacetic acid (8μL, 0.1 mmol) were mixed and degassed with N_2 for 15 min at room temperature. 15 mL of CH_2Cl_2 were added and the reaction mixture was stirred at room temperature for 1h. *p*-Chloranil (3.2 mmol, 790 mg) was then added and the mixture was stirred for further 15 min. The solution was dried under vacuum and chromatographed (silica gel, CH_2Cl_2) to give corrole **6** in 15% yield.

Anal. Calcd. for $C_{46}H_{50}N_4Si_3$: C, 74.34; H, 6.78; N, 7.54; Si, 11.34. Found: C, 74.24; H, 6.67; N, 7.42; Si, 11.28. UV-Vis (CH_2Cl_2): λ_{max}, nm 416, 567, 615, 648. ^{1}H NMR (300 MHz, $CDCl_3$), δ (ppm): 8.94 (d, *J* = 3.5 Hz, 4H, β-pyrrolic), 8.62 (d, *J* = 3.6 Hz, 4H, β-pyrrolic), 8.39 (d, *J* = 7.9 Hz, 4H, Ph), 8.20 (d, *J* = 8.1 Hz, 2H, Ph), 7.98 (d, *J* = 7.8 Hz, 4H, Ph), 7.93 (d, *J* = 7.9 Hz, 2H, Ph), 0.52 (s, 27H, CH_3 trimetylsilyl). MS (FAB): *m/z* 742.1 $[M]^+$.

10-(4-trimethylsilylphenyl)-5,15-dimesitylcorrole 7. The synthesis has followed an optimization of Gryko's reported procedure.[14] In a round bottom flask mesityldipyrromethane (2.57 mmol, 680 mg) and 4-trimethylsilylbenzaldehyde (1.28 mmol, 229 mg) have been dissolved in 250 mL of CH_3OH. Afterwards 6.3 mL of HCl_{aq} (36%w) in 125 mL of water was added and the solution was kept under stirring at room temperature for 2h. The mixture was extracted with 80 mL of $CHCl_3$, then the organic phase was washed 2 times with 80 mL of water, dried on sodium sulfate, filtered and diluted with 250 mL of $CHCl_3$. *p*-Chloranil (3.86 mmol, 947.86 mg) was added and the mixture was stirred overnight at room temperature. The reaction mixture was evaporated to dryness and chromatographed (silica gel, $CHCl_3$/Hexane, 3:1 v/v). All the fraction containing pure corrole were combined, evaporated and crystallized from CH_2Cl_2/CH_3OH 1:2 v/v affording pure **7** (465 mg, 18%).

Anal. Calcd. for $C_{46}H_{46}N_4Si$: C, 80.90; H, 6.79; N, 8.20; Si, 4.1. Found: C, 80.84; H, 6.58; N, 8.11; Si, 4.0. UV-Vis (CH_2Cl_2): λ_{max}, nm 408, 428, 566, 605, 635. ^{1}H NMR (300 MHz, $CDCl_3$), δ (ppm): 8.88 (d, *J* = 4.2 Hz, 2H, β-pyrrolic), 8.52 (d, *J* = 4.7 Hz, 2H, β-pyrrolic), 8.50 (d, *J* = 4.7 Hz, 2H, β-pyrrolic), 8.32 (d, *J* = 4.1 Hz, 2H, β-pyrrolic), 8.16 (d, *J* = 7.9 Hz, 2H, *meso* Ph), 7.87 (d, *J* = 7.9 Hz, 2H, *meso* Ph), 7.27 (s, 4H, *meso* Ph superimposed on $CHCl_3$ residual peak), 2.60 (s, 6H, CH_3 *para* Ph), 1.93 (s, 12 H, CH_3 *orto* Ph), 0.49 (s, 9H, CH_3 trimethylsilyl). ^{1}H NMR (300 MHz, DMSO-d_6) δ (ppm): 8.71 (d, *J* = 3.8 Hz, 2H, β-pyrrolic), 8.14 (d, *J* = 4.5 Hz, 2H, β-pyrrolic), 8.10-8.06 (dd superimposed, 2H, β-pyrrolic+2H *meso* Ph), 8.02 (d, *J* = 3.8 Hz, 2H, β-pyrrolic), 7.81 (d, *J* = 7.8 Hz, 2H, *meso* Ph), 7.22 (s, 4H, *meso* Ph), 2.52 (s, 6H, CH_3 *para* Ph superimposed on DMSO residual peak), 1.86 (s, 12H, CH_3 *orto* Ph), 0.45 (s, 9H, CH_3 trimethylsilyl). MS (FAB): *m/z* 682.1 $[M]^+$

[10-(4-trimethylsilylphenyl)-5,15-dimesitylcorrolato] phosphorus(V) 10. The synthetic protocol was based on a procedure reported in literature.[15] **7** (0,147 mmol, 100 mg) was dissolved in 8 mL of pyridine and degassed with N_2 for 15 minutes. The corrole solution was warmed to reflux and then an excess of $POCl_3$ (14,97 mmol, 1,4 mL) has been added keeping the reaction mixture under stirring and refluxing for 20 minutes. When the starting material was completely consumed, the reaction mixture was cooled in an ice bath, then water was added slowly (huge heat and fume releasing) till the formation of a precipitate. The reaction mixture was filtered on paper, washed with water, dried, dissolved with $CHCl_3$ and then chromatographed (silica gel, $CHCl_3/CH_3OH$ 99:1 v/v). All the fractions containing corrole **10** were collected, dried and then crystallized in CH_2Cl_2/CH_3OH 1:4 v/v affording the pure phosphorus corrole (105 mg, 96%).

Anal. Calcd. for $C_{46}H_{43}N_4PSi$: C, 77.72; H, 6.10; N, 7.88; P, 4.36; Si, 3.95. Found: C, 77.65; H, 6.03; N, 7.65; P, 4.24; Si, 3.76. UV-Vis ($CHCl_3$): λ_{max}, nm 409, 418, 525, 562, 595. ^{1}H NMR (300 MHz, $CDCl_3$+10%$_v$ CD_3OD), δ (ppm): 9.10 (dd, *J* = 4.2, 2.7 Hz, 2H, β-pyrrolic), 8.70 – 8.59 (m, 6H, β-pyrrolic), 8.14 (d, *J* = 7.7 Hz, 2H, *meso* Ph), 7.83 (d, *J* = 7.7 Hz, 2H, *meso* Ph), 7.25 (s, 4H, *meta* mesityl), 2.57 (s, 6H, CH_3 *para* Ph), 1.84 (s, 12H, CH_3 *orto* Ph, 0.45 (s, 9H, CH_3 trimethylsilyl). MS (FAB): *m/z* 1014.4 [M + 2 *m*-nitrobenzyl alcohol]$^+$

Sulfonation of [10-(4-trimethylsilylphenyl)-5,15-dimesitylcorrolato]phosphorous(V): The synthetic protocol was based on a procedure reported in the literature.[12] **10** (0.175 mmol, 130 mg) was dissolved in 35 mL of CCl_4 and degassed with N_2 for 15 minutes. The temperature was raised till refluxing, and then $ClSO_3Si(CH_3)_3$ (0.87 mmol, 135 μL) was added monitoring the progress of reaction by TLC (silica gel, $CHCl_3$). The reaction mixture was cooled at room temperature and then 26 mL of 1 M NaOH aqueous solution were added, and the solution was kept under stirring for 30 minutes. The organic phase of reaction mixture was separated from the aqueous phase. The aqueous phase was washed 3 times with 20 mL of $CHCl_3$, dried, dissolved with CH_3OH and chromatographed twice on a short plug (silica $CHCl_3/CH_3OH$ 20:80 v/v). The fraction containing corrole was dried and crystallized in CH_3OH/CH_2Cl_2 1:3 v/v affording **13** in 98% yield. The organic phase was chromatographed on a preparative TLC (silica, $CHCl_3/CH_3OH$ 98:2 v/v), separating a first fraction corresponding to **11** and a second one corresponding to **12**. The two product were crystallized in CH_3OH/CH_2Cl_2 1:2 v/v affording corrole **12** in 1% yield and corrole **11** in <1% yield.

11*:* Anal. Calcd. for $C_{45}H_{42}N_4O_5PS$: C, 69.13; H, 5.41; N, 7.17; O, 10.23; P, 3.96; S, 4.10. Found: C, 69.01; H, 5.31; N, 7.12; O, 10.16; P, 3.71; S, 4.09 UV-Vis ($CHCl_3$): λ_{max}, nm 409, 418, 522, 562, 595 ^{1}H NMR (300 MHz,

$CDCl_3$+10%$_v$ CD_3OD), δ (ppm): 9.10 (dd, 2H, β-pyrrolic), 8.65-8.60 (m, 6H, β-pyrrolic), 8.21 (s, 4H, *meso* Ph), 7.23 (s, 4H, *meta* mesityl), 2.56 (s, 6H, CH_3 *para* Ph), 1.85 (s, 12H, CH_3 *orto* Ph). MS (FAB): *m/z* 1021.2 [M + 2 *m*-nitrobenzyl alcohol]$^-$

12: Anal. Calcd. for $C_{48}H_{50}N_4O_5PSSi$: C, 67.50; H, 5.90; N, 6.56; O, 9.37; P, 3.63; S, 3.75; Si, 3.29. Found: C, 67.32; H, 5.88; N, 6.49; O, 9.25; P, 3.61; S, 3.65; Si, 3.27. UV-Vis ($CHCl_3$): λ_{max}, nm 409, 418, 522, 562, 593. ^{1}H NMR (300 MHz, $CDCl_3$+10%$_v$ CD_3OD), δ (ppm): 9.53 (s, 1H, β-pyrrolic), 8.76 (d, *J* = 3.4 Hz, 1H, β-pyrrolic), 8.61 – 8.42 (m, 5H, β-pyrrolic), 8.09 (d, *J* =7.6 Hz, 2H, *meso* Ph), 7.82 (d, *J* = 7.5 Hz, 2H, *meso* Ph), 7.23 (s, 2H, *meta* mesityl), 7.19 (s, 2H, *meta* mesityl) 2.56 (s, 3H, CH_3 *para* Ph), 2.53 (s, 3H, CH_3 *para* Ph), 1.84 (s, 6H, CH_3 *orto* Ph), 1.83 (s, 6H, CH_3 *orto* Ph) 0.44 (s, 9H, trimethylsilyl). MS (FAB): *m/z* 1093.2 [M + 2 *m*-nitrobenzyl alcohol]$^-$

13: Anal. Calcd. for $C_{45}H_{42}N_4O_8PS_2$: C, 62.71; H, 4.91; N, 6.50; O, 14.85; P, 3.59; S, 7.44. Found: C, 62.66; H, 4.86; N, 6.41; O, 14.67; P, 3.46; S, 7.32. 1H NMR (600 MHz, CD_3OD): δ, ppm 9.65 (dd, 3J(H,H) = 4.3 Hz, 4J(P,H) = 2.5 Hz, 1H; β-pyrrole H18), 8.76 (d, 4J(P,H) = 3.6 Hz, 1H; β-pyrrole H3), 8.67-8.64 (dd superimposed, 2H; β-pyrrole H7, H13), 8.65 (dd superimposed, 2H; β-pyrrole H8, H12), 8.58 (dd, 3J(H,H) = 4.2 Hz, 4J(P,H) = 3.5 Hz, 1H; β-pyrrole H17), 8.23-8.27 (dd, 3J(H,H) = 8.3 Hz, 4H; $ArSO_3H$ H27, H28), 7.33 (s, 4H; Ar H, H22), 2.61 (s, 6H; Ar p-CH_3, H24), 1.91 (s, 12H; Ar o-CH_3, H25); ^{31}P NMR (600 MHz, CD_3OD): δ, ppm -177.59. MS (FAB): *m/z* 551.0 [M+2 *m*-nitrobenzyl alcohol]$^{2-}$

Acknowledgements

This research has been supported by the University of Rome "Tor Vergata" (“Consolidate the Foundations” Chocolate project)

Keywords: porphyrinoids • corrole • sulfonation • phosphorus • scanning probe microscopy

[1] Z. Gross, N. Galili, I. Saltsman, *Angew. Chem., Int. Ed.* **1999**, *38*, 1427

[2] R. Paolesse, L. Jaquinod, D. J. Nurco, S. Mini, F. Sagone, T. Boschi, K. M. Smith, *Chem. Commun.* **1999**, 1307

[3] a) R. Paolesse, *Synlett* **2008**, 2215; b) C. M. Lemon, P. Brothers, *J. Porphyrins Phthalocyanines* **2011**, *15*, 809−834.

[4] a) C. M. Lemon, D. K. Dogutan, D. G. Nocera in *Handbook of Porphyrin Science Vol. 21* (Eds.: K. M. Kadish, K. M. Smith, R. Guilard), World Scientific Publishing, Singapore, **2012**, pp 1−143; b) H. Lei, H. Fang, Y. Han, W. Lai, X. Fu, R. Cao, *ACS Catal.* **2015**, *5*, 5145−5153.

[5] a) I. Luobeznova, M. Raizman, I. Goldberg, Z. Gross, *Inorg. Chem.* **2006**, *45*, 386−394; b) W. Shao, H. Wang, S. He, L. Shi, K. Peng, Y. Lin, L. Zhang, L. Ji, H. Liu, *J. Phys. Chem. B* **2012**, *116*, 14228−14234; c) J. F. B. Barata, A. Zamarrón, M. G. P. M. S. Neves, M. A. F. Faustino, A. C. Tomé, J. A. S. Cavaleiro, B. Röder, Á. Juarranz, F. Sanz- Rodriguez, *Eur. J. Med. Chem.* **2015**, *92*, 135−144.

[6] a) L. Tortora, G. Pomarico, S. Nardis, E. Martinelli, A. Catini, A. D'Amico, C. Di Natale, R. Paolesse, *Sens. Actuators B* **2013**, *187*, 72-77; b) R. Capuano, G. Pomarico, R. Paolesse, C. Di Natale, *Sensors*, **2015**, *15*, 8121-8130; c) X. B. Zhang, Z. X. Han, Z. H. Fang, G. L. Shen, R. Q. Yu, *Anal. Chim. Acta* **2006**, *562*, 210-215; d) J. Radecki, I. Stenka, E. Dolusic, W. Dehaen, *Electrochim. Acta* **2006**, *51*, 2282-2288; e) L. Lvova, C. Di Natale, A. D’Amico, R. Paolesse, *J. Porphyrins Phthalocyanines* **2009**, *13*, 1168–1178.

[7] J. F. B. Barata, C. I. M. Santos, M. G. P. M. S. Neves, M. A. F. Amparo, J. A. S. Cavaleiro in *Topics in Heterocyclic Chemistry, Synthesis and Modification of Porphyrinoids*, *Vol. 33,* (Ed.: R. Paolesse), Springer, New York **2014**, pp. 79–141.

[8] A. Mahammed, I. Goldberg, Z. Gross, *Org. Lett.* **2001**, *3,* 3443–3446.

[9] a) J. D. Sims, J. Y. Hwang, S. Wagner, F. Alonso Valenteen, C. Hanson, J. M. Taguiam, R. Polo, I. Harutyunyan, G. Karapetyan, K. Sorasaenee, A. Ibrahim, E. Marban, R. Moats, H. B. Gray, Z. Gross, L. K. Medina-Kauwe, *J. Control. Release* **2015**, *217*, 92-101; b) A. Preuß, I. Saltsman, A. Mahammed, M. Pfitzner, I. Goldberg, Z. Gross, B. Röder, *J. Photochem. Photob. B* **2014**, *133,* 39–46; c) Z. Okun, Z. Gross, *Inorg. Chem.* **2012**, *51*, 8083-8090.

[10] I. Saltsman, A. Mahammed, I. Goldberg, E. Tkachenko, M. Botoshanksy, Z. Gross, *J. Am. Chem. Soc.* **2002**, *124*, 7411-7420.

[11] M. L. Naitana, S. Nardis, S. Lentini, D. O. Cicero, R. Paolesse, *J. Porphyrins Phthalocyanines* **2015**, *19*, 1−10.

[12] a) G. Félix, J. Dunoguè, R. Calas, *Angew. Chem., Int. Ed.* **1979**, *18*, 402-404; b) B-H. Ye, Y. Naruta, *Tetrahedron* **2003**, *59*, 3593-3601.

[13] V. Král, P. Vašek, B. Dolenský, *Collect. Czech. Chem. Commun.* **2004**, *69*, 1126-1136.

[14] B. Koszarna, D.T. Gryko, *J. Org. Chem.* **2006**, *71*, 3707–3717.

[15] G. Pomarico, L. Tortora, F. R. Fronczek, K. M. Smith, R. Paolesse, *J. Inorg. Biochem*. **2016**, *158*, 17-23.

[16] a) M. Stefanelli, F. Mandoj, M. Mastroianni, S. Nardis, P. Mohite, F. R. Fronczek, K. M. Smith, K. M. Kadish, X. Xiao, Z. Ou, P. Chen, R. Paolesse, *Inorg. Chem.* **2011**, *50*, 8281–8292; b) M. Mastroianni, W. Zhu, M. Stefanelli, S. Nardis, F. R. Fronczek, K. M. Smith, Z. Ou, K. M. Kadish, Paolesse, R. *Inorg. Chem.* **2008**, *47*, 11680–11687.

[17] a) J. Mason in *Multinuclear NMR*; Plenum Press: New York, **1987**, 369; b) A. Ghosh, M. Ravikanth, *Chem. Eur. J.* **2012**, *18*, 6386−6396; c) A. Ghosh, W.-Z. Lee, M. Ravikanth, *Eur. J. Inorg. Chem.* **2012**, 4231–4239.

[18] a) T. Chatterjee, W.-Z. Lee, M. Ravikanth, *Dalton Transactions* **2016**, *45*, 7815-7822; b) J. Vestfrid, R. Kothari, A. Kostenko, I. Goldberg, B. Tumanskii, Z. Gross, *Inorg. Chem*. **2016**, *55*, 6061-6067; c) X. Liang, J. Mack, L.-M. Zheng, Z. Shen, N. Kobayashi *Inorg. Chem.* **2014**, *53*, 2797−2802.

[19] S. Nardis, F. Mandoj, R. Paolesse, F. R. Fronczek, K. M. Smith, L. Prodi, M. Montalti, G. Battistini, *Eur. J. Inorg. Chem.* **2007**, *16*, 2345-2352.

[20] V. M. Hallmark, S. Chiang, K.-P. Meinhardt, K. Hafner, *Phys. Rev. Lett.* **1993***, 70,* 3740-3743.

[21] A. F. Lee, K. Wilson, R. M. Lambert, A. Goldoni, A. Baraldi, G. Paolucci, *J. Phys. Chem. B* **2000**, *104*, 1172-11733.

[22] X. Miao, *Appl. Surf. Sci*. **2009***, 255,* 5885-5890.

[23] G. E. Poirier*, Langmuir*. **1997***, 13,* 2019-2026.

[24] C. Schonenberger, J. A. M. Sondag-Huethorst, J. Jorritsma, L. G. J. Fokkink, *Langmuir* **1994***, 10,* 611–614.

[25] A. E. Baber, S. C. Jensen, E. V. Iski, C. H. Sykes, *J. Am. Chem. Soc.* **2006***, 128,* 15384-15385.

[26] E. B. Stephens, K. E. Kinsey, J. F. Davis, J. M. Tour, *Macromolecules*, **1993**, *26*, 3519-3532

[27] P. G. Seybold, M. Gouterman, *J. Mol. Spectrosc.* **1969**, *31*, 1.

[28] A. Credi, L. Prodi, *J. Mol. Struc*. **2014**, *1077*, 30-39.

[29] R. Paolesse, A. Marini, S. Nardis, A. Froiio, D. J. Nurco, L. Prodi, M. Montalti, K. M. Smith, *J. Porphyrins Phthalocyanines* **2003**, 25–36.

Entry for the Table of Contents

FULL PAPER

Phosphorus is needed: The regioselective sulfonation of a triaryl corrole has been carried out with a novel strategy, where the phosphorus coordination has a “key role” in determining the corrole substitution pattern. The complex shows a high brightness in water, making it promising for sensor applications.

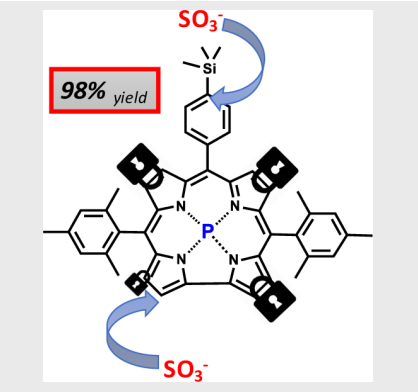

*Author(s), Corresponding Author(s)**

Page No. – Page No.

Title